IJTRET

International Journal of Trendy Research in Engineering and Technology
Volume 3 Issue 5 October 2019
ISSN NO 2582-0958

GROWTH AND OPTICAL CHARACTERIZATION OF FE DOPED BISMUTH TRIBORATE (FE- BIB_3O_6) CRYSTAL

P.Sureshkumar, M.Rathnakumari, J.Rajeev Gandhi,
So-Fi Infotech, Chennai-600099
Dept. of Physics, Saveetha School of Engineering, Chennai India

ABSTRACT

Fe doped orthorhombic Bismuth Triborate crystals have been grown by spontaneous nucleation method. The grown crystals were characterized morphology, EDX, FTIR, UV, Z-scan, SHG, photoluminescence and dielectric studies. The grown Fe doped BiB_3O_6 single crystal was confirmed orthorhombic (δ- BiB_3O_6) structure by morphology study. The presence of Fe in BiB_3O_6 was confirmed by the EDX analysis. The FTIR Spectrum was confirmed the functional groups. The cut of wavelength was observed from UV-Visible Spectrometer. The third order nonlinear optical property of Fe doped BiB_3O_6 crystal was studied by Z-scan technique using a cw (continuous wave) He-Ne laser wavelength of 632.8nm and power 15 mW. The third order nonlinear refractive index n_2 found to be $0.7796x10^{-9}cm^2/W$. The measured SHG value of Fe doped BiB_3O_6 crystal was 1.35 times higher than KDP crystal. The excitation and emission wavelength were observed from photoluminescence spectrum. The frequency dependent dielectric constant, dielectric loss and AC conductivity were studied in the frequency range of 100 Hz to 3 MHz.

Key words: Fe-BiB_3O_6crystal, Spontaneous nucleation method, Z- Scan, cw He-Ne Laser, SHG.

1. Introduction

Various main-group metal borates have been discovered and suggested for NLO applications, especially in UV region because of their high UV transmittance and high damage threshold. Besides, transition-metal borates and rare-earth metal borates integrating in one crystalline matrix with two or more physical features are also the focus of both theoretical and experimental studies. The presence of d- or f-block elements in these borates results in a variety of technologically important properties, and they emerge as important multifunctional materials when given optical characteristics are combined with magnetic or electric properties [1-5]. A combination of various attractive properties makes bismuth triborate, BiB_3O_6 (BIBO), a promising material for frequency conversion using phase matched second order nonlinear processes [6]. BIBO exhibits exceptionally high second order nonlinear susceptibility [7] which is associated with the contribution of the BiO_4 anionic group [8]. Phase diagram of stable compounds in the Bi_2O_3-B_2O_3 system has been well known since 1962 [9]. BiB_3O_6 was exhibit following phases;α-BiB_3O_6, β-BiB_3O_6, γ-$BiB_3O_6$and δ- BiB_3O_6. Monoclinic bismuth triborate α-BiB_3O_6 is very promising nonlinear crystal [10].

The studies of isovalent doping of monoclinic bismuth triborate with rare earths were done in order to obtain new laser materials for diode pumped lasers, but these studies revealed limited extend of doping that is insufficient for laser purposes[11,12]. Later, new polymorph of bismuth triborate, orthorhombic δ-BiB_3O_6 was discovered [13,14]. Nonlinear coefficients of δ- BiB_3O_6 are found to be rather high [15].

Transition metals doped glasses have found an interest in many areas of application. Such glasses are good materials for use in optical, electric, thermal, and mechanical applications. Transition metal ions are characterized by partially filled d-shell that can frequently exist in a number of oxidation states and the electro-optical behavior can occur as a result of electron transfers from ions in a lower to those in a higher oxidation state [16].The transition metals doped bismuth glasses show enhanced photoluminescence. These enhanced photoluminescence were observed due to energy transfer mechanism from the above ionic species to bismuth. In addition, bismuth containing glasses are used in the electronic field due to the low field strength and high polarizability of Bi^{3+} ions [17]. The distinctive optical absorptions due to electron transitions between the Fe^{3+} 3d levels had not been observed in their crystals probably due to low iron contents and the fact that such transitions in d_5 ions are spin forbidden. It has been reported that the spin forbidden d–d transitions of d5 ions could sometimes be observed in mineral crystals [18-23]. The optical absorption bands of these transitions are mostly in the visible and near infrared region.

In the present paper, we report the growth of Fe doped Bismuth triborate (δ- BiB_3O_6) crystal grown by

spontaneous nucleation method and Z-scan, SHG, photoluminescence, dielectric study and also crystal morphology studies.

2. Experimental procedure

2.1Growth

Starting materials of high purity Bi_2O_3, Fe_2O_3 and B_2O_3 (Sigma Aldrich) with the molar ratio 0.9:0.1:3 were taken in 50gm batch. The weighed materials were grounded and mixed by using mortar. The materials were loaded in platinum crucible and placed inside the electrical tubular furnace. The material was heated at 600º C for 5hrs further heating at 850º C for 8hrs. The material was melted at the time platinum wire was introduced in to the melt and stirred well for homogeneous solution. The homogenous solution was cooled to 600º C at the rate of 3C/hr. The material was placed inside the electrical furnace with heated at 850º C for 5hrs. The material was melted well for homogeneous solution then cooled to 710º C at the rate of 3ºC/hr. At that time platinum wire was introduced in to the homogeneous solution. The rotation speed of seed rod was 5 rpm and the cooling rate was 3ºC /day. The crystals were found to be nucleated around the seed rod and some of crystals nucleated on the surface of solution by spontaneous nucleation process. The rotation speed of seed rod was reduced from 5rpm to 3rpm because size of the crystals was increased.After 10 days the rod was pulled above the solution surface and cooled to 300º C at the rate of 3º C/hr. After this process furnace was switched off the crystals were reached to room temperature. The bunch of crystals grown around the platinum wire is shown in Fig. 1. The crystals were separated by mechanical fragmentation. Crystal of maximum size 5mm X 3mm was grown by this technique.

Fig.1. Bunch of orthorhombic Fe dopedBiB_3O_6 crystals

2.2 Characterization

Fe doped BiB_3O_6crystals grown by spontaneous nucleation method were subjected to single crystal X-ray diffraction studies was used by Bruker AxsKappaApex II CCD diffractometer. F E I Quanta FEG 200 - High Resolution Scanning Electron Microscope was used to EDS analysis for the determination of weight and atomic percentage. The optical absorption measurements were made using a Lambda 35 UV Winlab Spectrometer, in the range of 190 - 1100nm. Fourier Transform Infrared spectroscopy was carried out at room temperature in the range of 4000 – 450 cm^{-1}using a Perkin Elmer Spectrum two FT-IR/ ATR Spectrometer. The photoluminescence (PL) spectrum was recorded by Jobin Yvon spectrofluorometer (FLUOROLOG - FL3-11) with Xenon Lamp 450W as an excitation source in the range 180-1550 nm**.** The z-scan experimental technique was used to measure third order nonlinear optical properties. The second harmonic generation (SHG) efficiency of the sample was tested by Kurtz- Perry powder technique. The dielectric constant, dielectric loss and conductivity of the sample was measured in the frequency range of 50 Hz to 3 MHz at different temperatures by using Waynkerr Multi-component precision analyzer 6440B.

3. Results and Discussion

3.1 Crystal Morphology

Morphology of Fe dopedBiB_3O_6 single crystal has six well developed prominent planes (001), (010), (100), (00-1), (0-10), and (-100) which are shown in the Fig.2. The lattice parameters of the crystal are a = 4.266 Å, b = 4.439 Å, c=18.333 Å, $\alpha = \beta = \gamma = 90^o$ and V=347.18$Å^3$. The crystal phase was confirmed to be orthorhombic (δ- BiB_3O_6) and the space group symmetry is $Pca2_1$. The calculated lattice parameters of grown crystal were compared with reported values in Table 1.

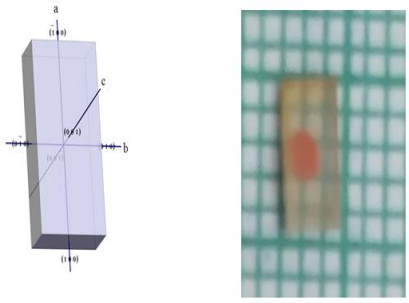

Fig.2. Morphology of δ- BiB_3O_6 crystal

Table 1. Unit cell parameters of Fe doped BiB_3O_6crystal

Parameters	Fe doped BiB_3O_6	Ref.[24]
a	4.266 Å	4.280 Å
b	4.439 Å	4.451 Å
c	18.333 Å	18.455 Å
$\alpha = \beta = \gamma$	90°	90°
V	347.18Å^3	351.57Å^3

3.2 EDX analysis of Fe doped BiB_3O_6crystals

Presence of Fe in BiB_3O_6 crystal was confirmed by the Energy dispersive X-ray analysis spectrum as shown in Fig.3. The information about the elemental weight and atomic percentage of the samples are shown in Table2.

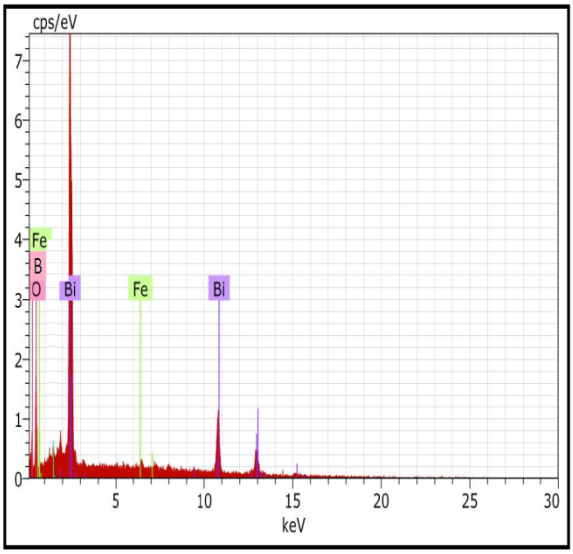

Fig. 3. EDX analysis of Fe dopedBiB_3O_6 Crystals

Elements	Weight %	Atom %
Bi	57.37	8.60
O	30.18	59.14
B	10.81	31.34
Fe	1.64	0.92
Total	**100.00**	**100.00**

Table 2.EDX analysis of Fe doped BiB_3O6Crystals

3.3 UV–Visible spectral analysis

The UV-Vis absorption spectrum is an essential tool to analyze the optical transmittance of the crystal. Absorption spectra are very important for any NLO material because, an NLO material can be practical use only if it has a wide transparency window. Fig.4 shows the optical absorption spectrum of Fe doped BiB_3O_6 Crystal. The lower cut off wave length is observed at 273nm. From the UV-spectrum it is seen that the crystal is found to be transparent in the region of 300-800 nm which is an essential parameter for frequency doubling process.Wide absorption band observed in the region 235-280nm. May be due to the doping of transition metal Fe in BiB_3O_6 which act as a activator [25, 26].

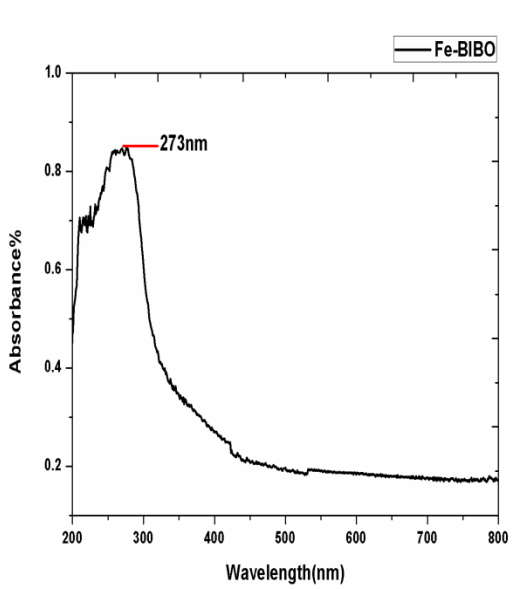

Fig.4 UV-Vis absorption spectrum of Fe doped BiB_3O6 Crystal

3.4 FTIR Spectrum analysis

The FTIR spectra revealed the presence of characteristic absorption bands for B_2O_3 and Bi_2O_3 of their various structural units. FTIR spectrum of Fe doped BiB_3O6 Crystals is shown in Fig 5. The absorption bands at 478 and 557cm^{-1}are specific to the vibrations of Bi–O bonds in BiO_6 octahedral units [27,28].The band at 598cm^{-1} is due to asymmetric stretching vibration of the B–O bonds in BO_4 units. The peak position at 756 cm^{-1} corresponds to B-O-B bending vibrations. The broad peaks at 869, 967, 1042, 1288 cm^{-1} corresponds to combined contribution of stretching vibrations of B-O bonds in BO_3 units from pyro-orthoborate groups and stretching vibration of B-O bonds in tetrahedral BO_4 units in tri-borate, tetra-borate and penta-borate groups. The bands at 1599, 1898, 1980, cm^{-1}are attributed to anti-symmetric stretching vibrations with three non-bridging oxygens (NBO's) of B-O-B groups. The peak at 478cm^{-1}can also be assigned to absorption band of Fe-O in octahedral structural units of Fe-O-OH [29]. The frequency assignments are shown in Table 3

Table3.FTIRassignments of Fe doped **BiB_3O6** Crystals

Position of absorptionbands (cm−1)	Assignment
478, 557	Vibrations of Bi–O bonds in BiO_6octahedral units, Fe–O in octahedral structural units of Fe-O-OH
598	Asymmetric stretching vibration of the B–O bonds in BO_4 units
756	B-O-B bending
869, 967, 1042, 1288	Stretching vibrations of B-O bonds in BO_3 units from pyro-orthoborate groups and stretching vibration of B-O bonds in tetrahedral BO_4 units in tri-borate, tetra-borate and penta-borate groups
1599, 1898, 1980	Anti-symmetric stretching vibrations with three non-bridging oxygens (NBO's) of B-O-B groups

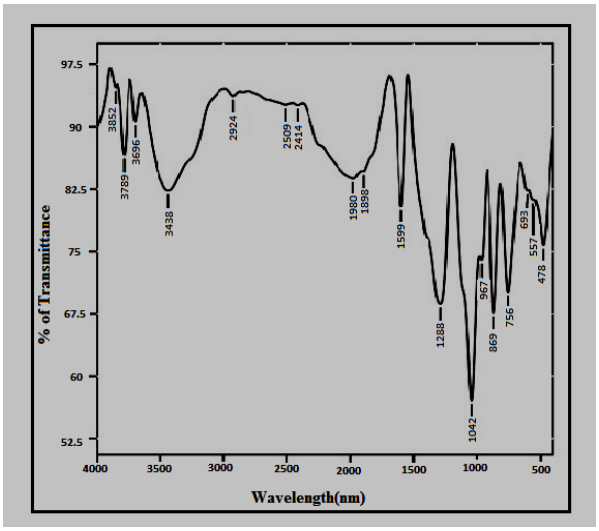

Fig.5. FTIR spectrum of Fe doped BiB_3O6Crystals

3.5 Third order nonlinear optical study

The third order nonlinear optical property of Fe doped BiB_3O_6 crystal has been studied by Z-scan technique using a cw (continuous wave) He-Ne laser wavelength of 632.8nm. The plots of normalized transmission and position of sample for Fe doped BiB_3O6 crystals are shown in Fig.6a and Fig.6b respectively for open and closed aperture setup. In this method, the sample is translated in the Z-direction along the axis of a focused Gaussian beam from the He-Ne laser at 632.8nm (15mW) and the far field intensity is measured as a function of the sample position. The intensity of incident laser beam (I_o) at the focus (Z=0) 3.13 MW/Cm^2. The magnitude of third order nonlinear optical susceptibility can be calculated by using the formula

$$\chi 3 = [\mathrm{Re}\,(\chi 3) + \mathrm{Im}\,(\chi 3)] \quad \ldots\ldots(1)$$

Where, Re (χ3), Im (χ3) are real and imaginary parts of third order susceptibility respectively can be obtained as

$$\mathrm{Re}\,(\chi 3) = 10^{-4}\varepsilon_o C^2 n_o^2 n_2/\pi\ (\mathrm{cm}^2/\mathrm{W}) \quad \ldots\ldots(2)$$

$$\mathrm{Im}\,(\chi 3) = 10^{-2}\varepsilon_o C^2 n_o^2 \lambda\beta/4\pi^2\ (\mathrm{cm}^2/\mathrm{W}) \quad \ldots\ldots(3)$$

The real part of nonlinear susceptibility is directly proportional to the nonlinear refractive index, and imaginary part of susceptibility is directly proportional to the nonlinear absorption. The nonlinear absorption and nonlinear refractive index of the crystal has been measured by open and closed aperture methods respectively. The nonlinear refractive index is given by the relation

$$n_2 = \frac{\Delta\Phi}{KI_oL_{eff}} \quad \ldots\ldots(4)$$

Where $\Delta\Phi$ is the nonlinear phase shift in terms of normalized transmittance, $K = 2\pi/\lambda$ (λ is the wave length of laser beam), I_o is the intensity of the laser beam and L_{eff} is the effective thickness of the sample. The nonlinear refractive index and magnitude of nonlinear susceptibility are listed in Table4.

Table 4. Z-scan technique measurement data of Fe doped BiB_3O_6 Crystal

Optical parameters	Values
Nonlinear absorption coefficient (β)	4.7604×10^{-5}cm/W
Nonlinear refractive index (n_2)	$1.18277\times10^{-10}cm^2/W$
Real part of the third order susceptibility Re(χ^3)	0.951764×10^{-12}(esu)
Imaginary part of the third order susceptibility Im(χ^3)	0.19298×10^{-9}(esu)
Third order nonlinear susceptibility (χ^3)	0.19393×10^{-9}(esu)

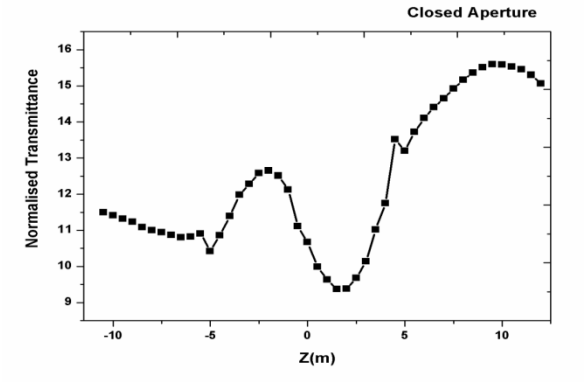

Fig.6a closed aperture Z-scan measurement of Fe doped BiB_3O_6 crystal

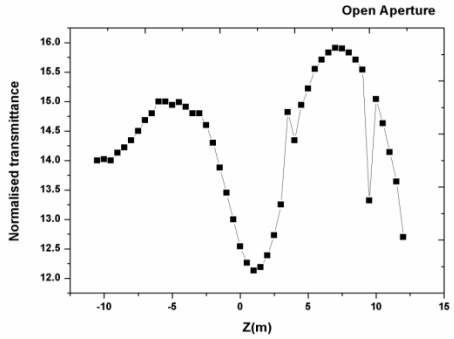

Fig.6b open aperture Z-scan measurement of Fe doped BiB_3O_6 crystal

3.6 Second order nonlinear optical study

The second harmonic generation (SHG) efficiency of the sample BiB_3O_6 was tested by Kurtz-Perry powder technique. The crystal was ground to homogeneous powder and tightly packed in a micro capillary tube and mounted in the path of the Q-switched Nd :YAg laser beam emitting wave length 1064 nm with pulse energy of 1.2mJ/pulse, pulse width of 8 ns and repetition rate of 10 Hz. The Fe doped BiB_3O_6 crystal gave a signal of 23 mV/pulse. The reference inorganic KDP crystal gave a signal of 17 mV/pulse for the same input energy. This result indicates that the grown crystal has SHG energy conversion efficiency 1.35 times higher than that of the inorganic standard KDP.

3.7 Photoluminescence

As seen in Fig. 7, the Photoluminescence spectrum was recorded in the range of 200 – 460nm. The excitation band of material Fe doped $BiB_3O_6$was observed at 294 nm, which is assigned to the $z\ ^6F^\circ_{9/2} \rightarrow a\ ^4D_{7/2}$ transition. The emission band was observed at 369 nm from the $a^4D_{7/2} \rightarrow z\ ^6F^\circ_{9/2}$ upon excitation with 294 nm. The emission band of doped BiB_3O_6 lies between 320 nm to 450 nm which is in the UV-blue region.

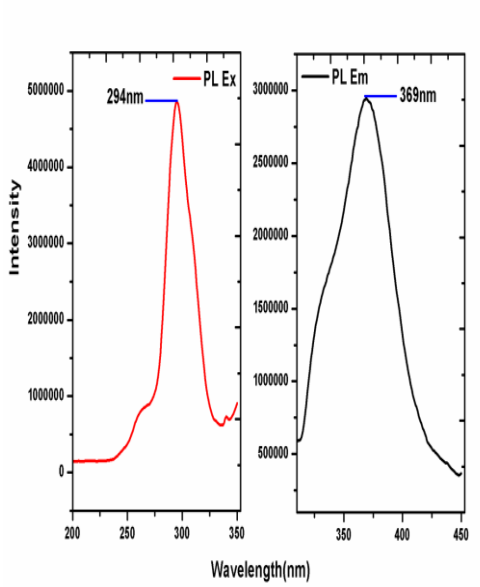

Fig.7 Photoluminescence Excitation and Emission Spectrum of Fe doped BiB_3O6crystal.

3.7 Dielectric Studies

Dielectric study is essential for nonlinear optical materials, to find how easily the materials are polarized in an electric field [30]. Frequency dependence of dielectric constant, dielectric loss and AC conductivity for Fe doped BiB_3O_6 crystals were carried out at varies temperatures from 305 K to 473 K in the frequency range of 100 Hz to 3 MHz. The following formula was used to calculate the dielectric constant,

$$\varepsilon_r = \frac{Cd}{A\varepsilon_0}$$

Where, C is the capacitance of the sample, d is sample thickness, A is surface area of the sample, ε_0- is permittivity of free space (8.854×10^{-12}F/m).The dielectric constant of Fe doped BiB_3O_6 crystals was large at low frequency as shown in Fig.8 due to the involvement of ionic, electronic, dipolar, orientation and space charge polarization which are active at low frequencies. It decreases with increasing frequency. This behavior is a general trend for the dielectric materials due to the scattering of charge carriers at high frequencies as well as the fast variation of the

electric field accompanied with the frequency. This process leads to random orientation of the dipole moments and hence decreases the value of dielectric constant(ε_r)[31].The dielectric permittivity in Fe doped BiB_3O_6 crystal is closely associated with the polarization of cations and anions, related to the electron polarization and ionic polarization under an electric field (the Bi–O octahedrons, B(1)–O tetrahedrons and B(2)–O trigons all contribute to the polarizations,[32] here we just discuss the Bi–O octahedrons due to their strong distortion and the lone-pair electrons of Bi^{3+}).[33]

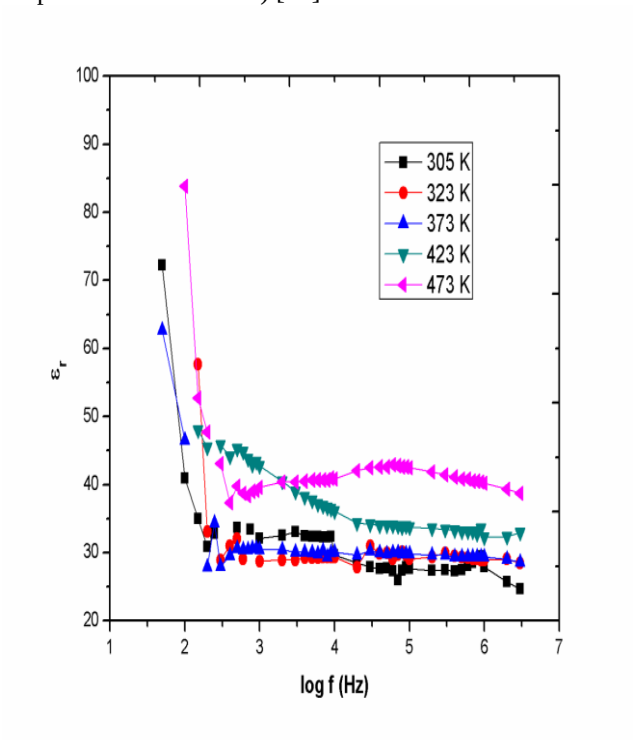

Fig. 8 Frequency dependence dielectric constant of Fe doped BiB_3O_6 crystal

Fig. 9 shows the frequency dependence of dielectric loss (tan α) of Fe doped BiB_3O_6 crystal. Dielectric loss of Fe doped BiB_3O_6 crystal is nearly zero at higher frequencies and it found to increase with increase in temperature. This may be due to the reason that at low temperature, the role of impurities in polarization of the material is negligible, but it becomes significant when the temperature is increased (Rahman et al.2012).

The AC conductivity (σ_{ac}) of the sample was calculated from the following equation,

$$\sigma_{ac} = \omega\varepsilon_r\varepsilon_o\tan\delta$$

Where $\omega=2\pi f$ is the angular frequency, f is the applied frequency. Figure 3 shows the frequency dependent AC conductivity (σ_{ac}) of Fe doped BiB_3O_6 crystal at various temperature from 305 K to 473 K. AC conductivity of Fe doped BiB_3O_6 crystal is nearly zero at lower frequency up to 100K Hz and found to increase thereafter. In general the high conductivity behavior for the sample at higher frequencies confirms the short range intrawell hoping of charge carriers between localized states [34]

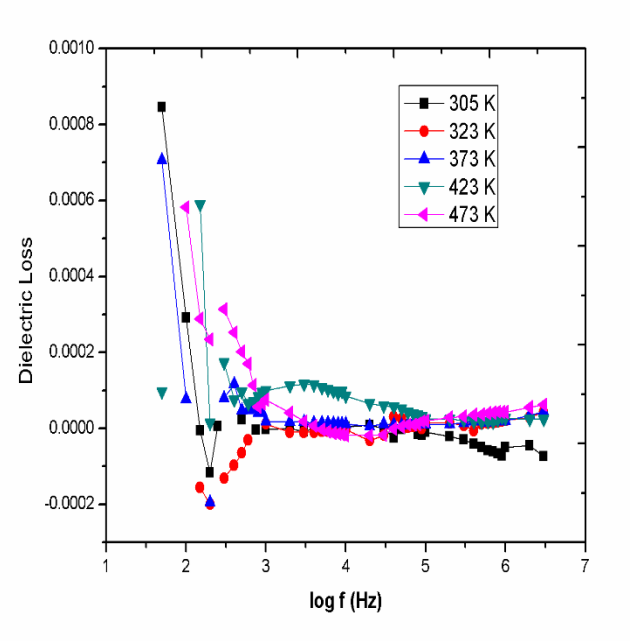

Fig.9 Frequency dependence Dielectric loss of Fe doped BiB_3O_6 crystal

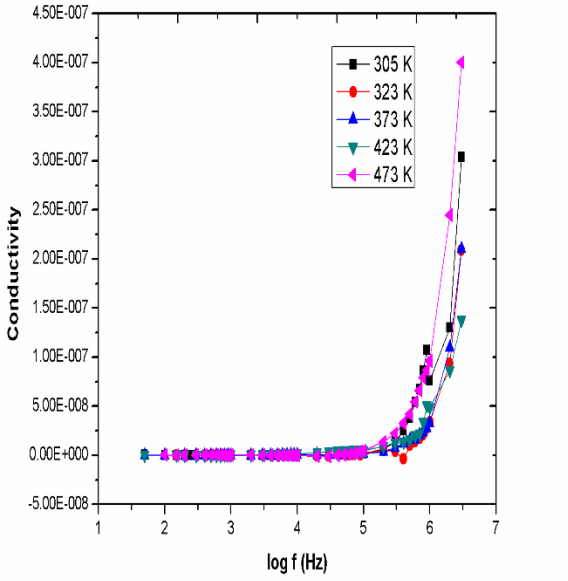

Fig 10 Frequency dependence AC conductivity of Fe doped BiB_3O_6 crystal

4. Conclusion

The Fe doped Bismuth triborate crystals have been grown by spontaneous nucleation method. The grown crystals were morphology for confirmation of crystal structure lattice parameters. The functional groups of grown crystal were identified by the FTIR spectral analysis. From UV-visible NIR absorption spectra was used to find cut off wave length. The EDS analysis was used to calculate the percentage of elements. The Photoluminescence excitation and emission spectrum was recorded. The third order nonlinear refractive index studied by Z-scan technique using CW He-Ne laser wavelength of 632.8nm. The measured SHG value is 1.35 times higher than KDP crystal. The dielectric constant of Fe doped BiB_3O_6 crystal was stable at higher frequencies and it increase with increasing temperature.

Acknowledgement:

The authors wish to thank Department of Science and Technology for the financial support to carry out this work (Project sanction number: SB/S2/LOP-0003/2013).

Referances

1.N.I. Leonyuk, L.I. Leonyuk, Prog. Cryst.Growth Charact.31 (1995) 179.

2.A.D. Mills, Inorg. Chem. 1 (1962) 960.

3.D.A. Keszler, Curr. Opin.Solid State Mater.Sci.1 (1996) 204.

4.K.N. Boldyrev, E.P. Chukalina, N.I. Leonyuk, Phys. Solid State 50 (2008) 1681.

5. E.A. Popova, N.I. Leonyuk, Phys. Rev. B 76 (2007) 054446.

6. P. Tzankov and V.Petrov, "Effective second order nonlinearity in acentric optical crystalswith low symmetry," Appl. Opt. 44, 6971-6985, 2005.

7. Hellwig, J. Liebertz, and L. Bohaty, "exceptional large nonlinear optical coefficients in the monoclinic Bismuth borate BiB_3O_6 (BIBO)," Solid state Commun.109, 249-251, 1999.

8. Zh. Lin, Zh. Wang, C. Chen and M-H. Lee, Mechanism of linear and nonlinear optical effects in monoclinic bismuth borate (BiB_3O_6) crystal," J. Appl. Phys. 90, 5585-5590, 2001.

9. E.M. Levin, C.L. McDaniel, J.Am. Ceram.Soc. 45 (1962) 335.

10. V. Petrov, M. Ghotbi, O. Kokabee, A. Esteban-Martin, F. Noack, A. Gaydardzhiev, I. Nikolov, P. Tzankov, I. Buchvarov, K. Miyata, A. Majchrowski, I.V. Kitky, F. Rotermund, E. Michalski, M. Ebrahim-Zadeh, Laser & Photon. Rev.4 (2010) 53.

11. A. Brenier, I. Kityk, A. Majchrowski, Opt. Commun. 203 (2002) 125.

12. P. Becker, C. Wickleder, Cryst. Res. Technol. 36 (2001) 27.

13. A.I. Zaitsev, A.D. Vasiliev, in: Proc. Symp. Order disorder and properties of oxides ODPO-9, Rostov-on-Don-loo, Russia, 19-23, September 2006, pp. 151.

14. J.S.Knyrim, P. Becker, D. johrendt, H. Huppertz, Angew. Chem. Int.Ed. 45(2006) 8239.

15. A.V. Cherepakhin, A.I. Zaitsev, A.S. Aleksan-drovsky, A.V. Zamkov, opt. Mater. 34 (2012) 790.

16. Sahar MR, Budi AS. Optical band gap and IR spectra ofglasses in the system [Nd2O3](*x*)–[CuO](35−*x*)–[P2O5](65). SolidStateSciTechnol 2006;14:115–20.

17. Pan A, Ghosh A. A new family of lead–bismuthate glass witha large transmitting window. J Non-Cryst Solid2000;271:157–61.

18. R.L. Greene, D.D. Sell, W.M. Yen, A.L. Schawlow, Phys. Rev. Lett. 15 (1965) 656.

19. W.H.J. Stork, G.T. Pott, J. Phys. Chem. 78 (1974) 2496.

20. R. Heitz, A. Hoffmann, I. Broser, Phys. Rev. B 45 (1992) 8977.

21. R.K. Moore, W.B. White, Can. Mineral. 11 (1972) 791.

22. Y. Tanabe, S. Sugano, J. Phys. Soc. Jpn. 9 (1954) 753.

23. N.T. Melamed, P.J. Viccaro, J.O. Artman, F.S. Barros, J. Lumin. 1&2 (1970) 348.

24. D.A.Ikonnikov, A.V.Malakhovskii, A.L.Sukhachev, A.I.Zaitsev, A.S.Aleksandrovsky, V.Jubera, spectroscopic properties of Nd3+ in

orthorhombic δ- BiB_3O_6 crystal. Optical Materials 34 (2012) 1839-1842

25. ElBatal, F.H., El Kheshen, A.A., Azooz, M.A. & Abo-Naf, S.M. 2008. Gamma ray interaction with lithium diborate glasses containing transition metals ions. *Optical Materials* 30: 881-891.

26. Moistafa, F.A., Fayad, A.M., Ezz-Eldin, F.M. & El-Kashif, I. 2013. Effect of gamma radiation on ultraviolet, visible and infrared studies of NiO, Cr2O3 and Fe2O3-doped alkali borate glasses. *Journal of Non-Crystalline Solids* 376: 18-25.

27. A.H. Doweidar, Y.B. Saddeek, J. Non-Cryst. Solids 355 (2009) 348.

28.M. Bosca, L. Pop, G. Borodi, P. Pascuta, E. Culea, J. Alloys Compd. 479 (2009) 579.

29. D.M.D. Caki´ c, G.S. Nikoli´ c, L.A. Ili ´ c, Bull. Chem. Technol. Macedonia 21 (2002)135.

30. Boyd RW. Nonlinear optics. 3rd ed. (UK) Elsevier publications: 2011.

31. Rajeev ganthi J. Influence of metal ion doping on Dielectric, ionic conductivity and piezo electric properties of flux grown KTP crystals. J.Alloys and compounds.

32. O.Schmidt, S. Gorfman and U. Pietsch, Cryst. Res. Technol., 2008, 43, 1126.

33. R. E. Newnham, Properties of Materials: Anisotropy, Symmetry,Structure, Oxford University Press, NY, 2005, pp. 58–98.

34. A.K. Abdul Gafoor, M.M. Musthafa, P.P. Pradyumnan "Edffect of Nd 3+ Doping on optical and dielectric properties of Tio2 Nanoparticles Synthesized by a low Temperature Hydrothermal method" Jr of Nanoscience and Nano technology 1,53-57 (2012).